VSP

Journal of Biomaterials Science 23 (2012) 1185–1198

Journal of BIOMATERIALS SCIENCE
brill.nl/jbs

Electrospun Biomimic Nanofibrous Scaffolds of Silk Fibroin/Hyaluronic Acid for Tissue Engineering

Kuihua Zhang [a], **Linpeng Fan** [b], **Zhiyong Yan** [a], **Qiaozhen Yu** [a] **and Xiumei Mo** [b,*]

[a] College of Materials and Textile Engineering, Jiaxing University, Zhejiang 314001, P. R. China

[b] Biomaterials and Tissue Engineering Lab, College of Chemistry and Chemical Engineering and Biological Engineering, Donghua University, Shanghai 201620, P. R. China

Received 13 January 2011; accepted 30 April 2011

Abstract

This study aimed to fabricate nanofibrous scaffolds which could biomimic the natural extracellular matrix from aqueous solutions of silk fibroin and hyaluronic acid blends (SF/HA) by means of electrospinning. Scanning electronic microscopy results indicated that electrospun SF/HA nanofibers were ribbon-shaped and their average width obviously decreased with the increase of HA content. However, there is no fiber observed when the volume of HA further increased to 50% of overall volume. After being treated with 75% ethanol vapor for 24 h, the fibers still remained their fibrous morphologies and presented good capability of water-resistance. Fourier transform infrared attenuated total reflectance spectroscopy, ^{13}C-CP-MAS nuclear magnetic resonance and differential scanning calorimetry results revealed that HA did not induce SF conformation from random coil to β-sheet. SF conformation converted from random coil to β-sheet after being treated with 75% ethanol vapor. Cell viability studies demonstrated that SF/HA nanofibrous scaffolds significantly promoted cell proliferation. Electrospun SF/HA nanofibers may provide an ideal biomimic tissue-engineering scaffold or vehicle for water-soluble drugs.

Keywords

Electrospinning, silk fibroin, hyaluronic acid, nanofibrous scaffolds

1. Introduction

One of the most significant objectives in tissue-engineering research is to design and obtain scaffolds with the capability of biomimicking the natural extracellular matrix (ECMs) from chemical composition, physical structure and biological functions [1, 2]. Natural extracellular matrix (ECM) is composed of a cross-linked porous network of multifibril collagens with diameters ranging from 50 to 500 nm and embedded in glycosaminoglycans [3, 4]. In order to mimic the porous structure of

* To whom correspondence should be addressed. E-mail: med@dhu.edu.cn

DOI:10.1163/092050611X576963

natural ECMs, electrospinning was applied to produce nanofibrous scaffolds from biodegradable polymers [5, 6].

Electrospinning utilizes electric force to drive the spinning process and produce fibers from polymer solutions or melts. This technique has been used as an efficient processing method to manufacture fibers with nanoscale diameters. Meanwhile, electrospun nanofibrous scaffolds have inherently high porosities and surface-area-to-volume ratios, and resemble the topographic features of the ECMs to encourage cell adhesion, proliferation or differentiation [5]. Many biodegradable synthetic and/or natural polymers have been electrospun into nanofibrous scaffolds for various tissues repair and regeneration, such as bone, cartilage, vascular blood, nerve, skin and bladder [2, 6–8].

Silk fibroin (SF) is an attractive natural fibrous protein for biomedical applications due to its unique properties, including good biocompatibility and biodegradability, low inflammatory response and commercial availability at relatively low cost [9, 10]. For tissue engineering applications, SF has been successfully explored for application in scaffolds of skin, bone, cartilage, vascular blood and never repair [11, 12]. Hyaluronic acid (HA) is a linear polysaccharide consisting of alternating disaccharide units of (1,4)-linked α-D-gluconic acid and (1,3)-linked β-N-acetyl-D-glucosamine. As one of the main components of the ECM, it is conducive to maintaining the architecture and visco-elastic properties of tissue and modulating cell functions such as adhesion, migration and proliferation [13]. Because of excellent biocompatibility and biodegradability, HA and its derivatives have been extensively used in biomedical areas including serving as tissue-engineering scaffolds, wound dressings, drug-delivery systems and implant materials [7]. Recently, SF/HA cardiac patches and freeze-drying porous scaffolds have been developed that enhance human mesenchymal stem cell growth [14, 15]. Electrospun SF/HA nanofibrous scaffolds may be ideal materials for tissue engineering due to their ability to biomimick ECM from components to architecture.

SF has been electrospun with spinning solvents such as hexafluoro-2-propanol (HFIP) [16, 17], hexafluoroacetone (HFA) [18], formic acid [19] and water [20]. In our previous study, nanofibers were successfully fabricated by electrospinning from the aqueous solutions of SF, and the resultant SF nanofibrous mats showed good cyctocompatibility to animal cells [21]. However, because of the high viscosity and surface tension of an aqueous HA solution, electrospinning of HA aqueous solution is very difficult. Um *et al.* [22] fabricated nanofibrous mats from HA aqueous solutions by a new electro-blowing process using the combination of air-flow and electrospinning techniques. Water is an ideal solvent for both fabrication processes and biomedical applications of the scaffolds. The electrospinning of aqueous solutions not only avoids the presence of a trace of toxic organic solvents or acids in electrospun scaffolds to affect cell growth, but also is beneficial in fabricating functional nanofibrous scaffolds containing water-soluble materials, such as various growth factors, water-soluble vitamin and water-soluble drugs.

In the present study, SF/HA nanofibrous scaffolds were successfully fabricated from their aqueous solutions *via* electrospinning. The morphology and structure of the electrospun nanofibers and the nanofibers treated with 75% ethanol vapor were also investigated. To assess the cytocompatibility and cells behavior on electrospun scaffolds, interaction between electrospun SF/HA nanofibrous scaffolds and pig iliac endothelial cells (PIECs) was studied.

2. Materials and Methods

2.1. Materials

Cocoons of *Bombyx mori* silkworm was kindly supplied by Jiaxing Silk. Hyaluronic acid (sodium salt, Mw = 200 000) was purchased from Dali.

Pig iliac endothelial cells (PIECs) were obtained from institute of biochemistry and cell biology (Chinese Academy of Sciences). Except specially explained, all culture media and reagents were purchased from Gibco Life Technologies.

2.2. Preparation of Regenerated SF

Raw silk was degummed three times with 0.5% (w/w) Na_2CO_3 solution at 100°C for 30 min each and then washed with distilled water. Degummed silk was dissolved in a ternary solvent system of $CaCl_2/H_2O$/EtOH solution (1:8:2 mol ratio) for 1 h at 70°C. After dialysis through a cellulose tubular membrane (250-7u; Sigma) in distilled water for 3 days at room temperature, the SF solution was filtered and lyophilized to obtain the regenerated SF sponges.

2.3. Electrospinning

The regenerated SF sponges and HA were dissolved in distilled water for 30 wt% SF solution and 4 wt% HA solution, respectively. When they were prepared, the two solutions were blended at different volume ratios with sufficient stirring at room temperature before electrospinning. The solutions were placed into a 2.5 ml plastic syringe with a blunt-ended needle with an inner diameter of 0.21 mm. The needle was located at a distance of 15 mm from the grounded collector. A syringe pump (789100C, Cole-Parmer) was employed to feed solutions to the needle tip at a feed rate of 0.5 ml/h. A high electrospinning voltage was applied between the needle and ground collector using a high voltage power supply (BGG6-358, Bmeico). The applied voltage was 20 kV.

2.4. Characterization

The morphology and diameter of the electrospun fibers was observed with a scanning electronic microscope (SEM, JSM-5600) at an acceleration voltage of 10 kV. The diameter range of the fabricated ultrafine fibers was measured based on the SEM images using the image visualization software Image-J 1.34s (National Institutes of Health) and calculated by selecting 100 fibers randomly observed on the SEM images.

Fourier transform infrared attenuated total reflectance spectroscopy (FT-IR–ATR) spectra were obtained at room temperature on an Avatar 380 FT-IR instrument (Thermo Electron) in the range 4000–600 cm^{-1} at a resolution of 4 cm^{-1}.

^{13}C-CP-MAS-NMR spectra of SF scaffolds were obtained on a NMR spectrometer (Bruker AV400) with a ^{13}C resonance frequency of 100 MHz, contact time of 1.0 ms and pulse delay time of 4.0 s.

Thermographs were acquired using a differential scanning calorimeter (DSC, TA Instruments) from room temperature to 350°C at a rate of 10°C/min under a nitrogen atmosphere. The nitrogen gas flow rate was 40 ml/min.

The surface tensions of the SF/HA blended solutions with different volume ratios were measured with a surface tension analyzer (BZY, Shanghai Ruifang Instrument). Every sample was measured 3 times.

2.5. Treatment of Electrospun Nanofibrous Scaffolds

SF and SF/HA blended nanofibrous scaffolds were treated with 75% (v/v) ethanol vapor to induce a β-sheet conformational transition, which results in insolubility in water. Briefly, 75% (v/v) ethanol vapor-treated samples were prepared by placing SF and SF/HA nanofibrous scaffolds in a desiccator saturated with 75% (v/v) ethanol vapor at room temperature for 24 h and then dried in a vacuum at room temperature for 1 week.

2.6. Cell Viability Assay on Nanofibrous Scaffolds

Pig iliac endothelial cells (PIECs) were cultured in DMEM medium with 10% fetal bovine serum and 1% antibiotic–antimycotic in an atmosphere of 5% CO_2 and 37°C, and the medium was replenished every three days. SF nanofibrous scaffolds were deposited on circular glass cover slips (14 mm in diameter) for cell study. The 75% ethanol vapor treated nanofibrous scaffolds were placed in 24-well cell-culture plate with no further sterilization for the cell-viability assay.

Cell viability on electrospun scaffolds and coverslips (control) and tissue culture plates (TCP) (control) was determined by the MTT method. Briefly, the cell and electrospun scaffolds, coverslips and TCP were incubated with 5 mg/ml 3-[4,5-dimehyl-2-thiazolyl]-2, 5-diphenyl-2H-tetrazolium bromide (MTT) for 4 h. Thereafter, the culture media were extracted and 400 µl dimethylsulfoxide (DMSO) was added for about 20 min. When the crystals were sufficiently resolved, aliquots were pipetted into the wells of a 96-well plate and tested by an enzyme-labeled Instrument (MK3, Thermo), and the absorbance at 490 nm of each well was measured.

For the proliferation study, endothelial cells were seeded onto fiber scaffolds and control glass cover slips ($n = 3$) at a density of 1.43×10^4 cells/well for 1, 3, 5 and 7 days. After cell seeding, unattached cells were washed out with PBS solution and attached cells were quantified by the MTT method.

After 3 days of culturing, the electrospun fibrous scaffolds with cells (density 1.43×10^4 cells/well) were examined by SEM. The scaffolds were rinsed twice with

PBS and fixed in 4% glutaraldehyde water solution at 4°C for 2 h. Fixed samples were rinsed twice with PBS and then dehydrated in graded concentrations of ethanol (30, 50, 70, 80, 90, 95 and 100%). Finally, they were dried in vacuum overnight. The dry cellular constructs were coated with gold sputter and observed under the SEM at a voltage of 10 kV.

2.7. Statistical Analysis

Statistical analysis was performed using Origin 7.5 (Origin Lab). Statistical comparisons were determined by one-way ANOVA. In all evaluations, $P < 0.05$ was considered as statistically significant.

3. Results and Discussion

3.1. Morphology of SF/HA Nanofibers

The SEM micrographs of electrospinning of 30 wt% SF/4 wt% HA blend solutions with different volume ratios and average widths of nanofibers are shown in Fig. 1. When the volume ratios of 30 wt% SF/4 wt% HA blend solutions were 10:0, 8:2, 6:4 and 5:5, respectively, ribbon-shaped electrospun fibers were observed. According to Koombhongse *et al.* [23], ribbon-shaped fibers are obtained due to the formation of a thin polymer shell on the surface of the cylindrical fluid jet between the electrodes. The solvent evaporates after shell formation, atmospheric pressure causes a collapse of the cylindrical jet and the fibers change first into an elliptic and then into a flat shape. Incomplete fiber drying also leads to the formation of ribbon-like (or flattened) fibers as compared to fibers with a circular cross section. Meanwhile, the width of nanofibers gradually decreased with the increase of HA content. When the volume ratio of SF/HA blend solutions was less than 5:5, continuous fibers did not appear. Particular to pure HA solution, only beads were produced. As HA is a polyanionic electrolyte, the unusually high viscosity and the surface tension of HA hinders the electrospinning process [22]. Figure 2 shows the surface tension of SF/HA blend aqueous solutions with different volume ratios. Pure HA aqueous solution had an extra high surface tension (68.63 ± 1.14 mN/m). The surface tension of pure SF aqueous was 43.27 ± 0.15 mN/m. At the beginning, the surface tension of SF/HA blend aqueous solutions slightly decreased with the increase of HA content. When the volume ratio was less than 5:5, the surface tension of SF/ HA blend aqueous solutions gradually increased. This may be one reason that SF/HA blend solution cannot be electrospun when the volume ratio was less than 5:5. In addition, the addition of HA to SF solutions could result in an increase of ion strength, which might produce higher conductivity. Much higher charge density was not beneficial to electrospinning process. The increased charge density will increase elongation forces, which exert on the fiber jet to yield a smaller fiber [24]. Therefore, we found nanofibers width decreased with HA content increasing.

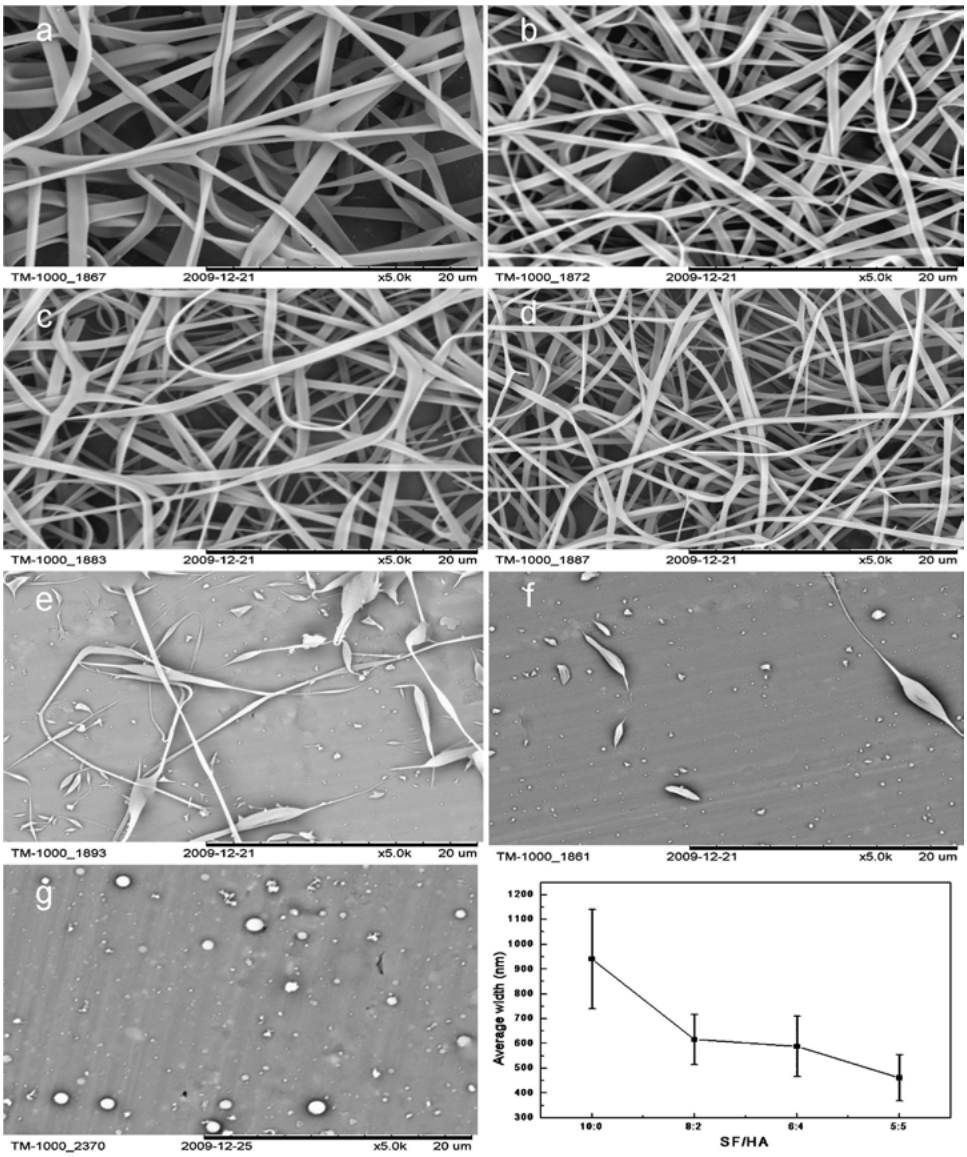

Figure 1. SEM images and width of SF/HA blend nanofibers with different volume ratios. (a) 10:0; (b) 8:2; (c) 6:4; (d) 5:5; (e) 4:6; (f) 2:8; (g) 0:10.

3.2. Post-Treatment of SF/HA Nanofibers

The electrospun SF/HA blend nanofibers are soluble in water. To potentially use electrospun SF/HA fibers for tissue engineering, post-treatment is necessary. Electrospun pure SF nanofibrous scaffolds were treated with methanol, ethanol or water vapor to improve stability both *in vivo* and *in vitro* [25, 26]. In the experiment, we used 75% (v/v) ethanol vapor as post-treatment of electrospun SF/HA fibers. Fig-

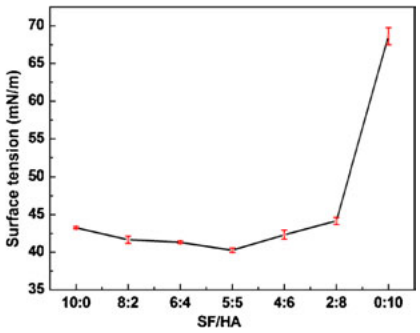

Figure 2. Surface tensions of SF/HA blend aqueous solutions with different volume ratios. This figure is published in colour in the online edition of this journal, which can be accessed *via* http://www.brill.nl/jbs

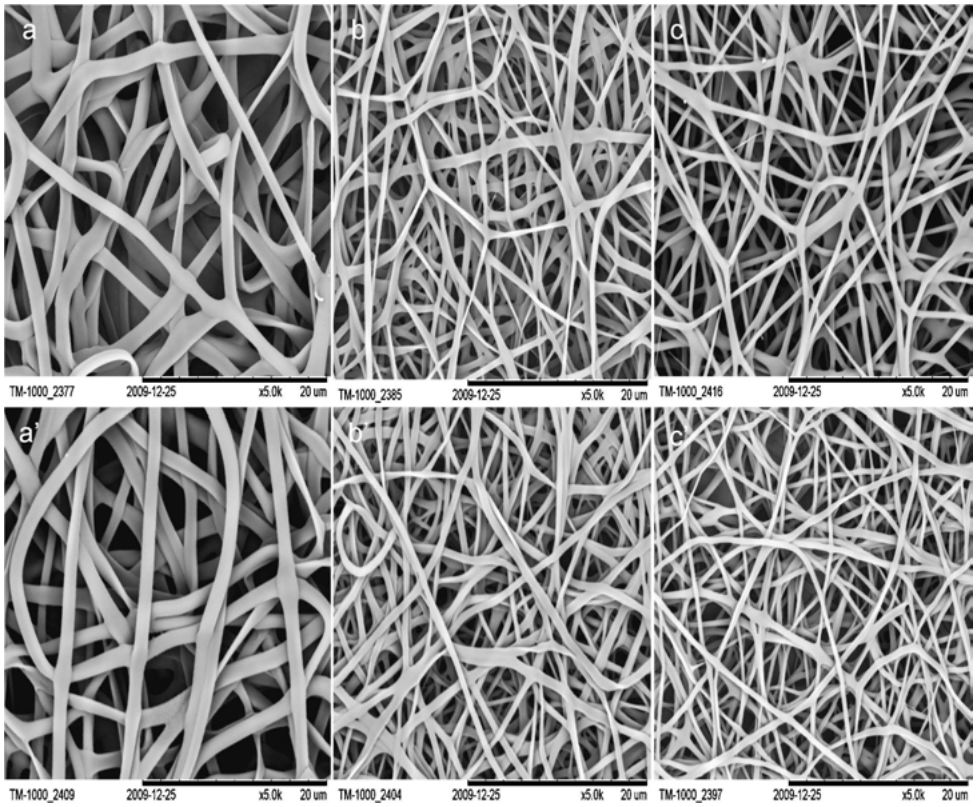

Figure 3. SEM photographs of SF/HA nanofibrous scaffolds after treatment with 75% (v/v) ethanol vapor and being soaked in deionized water for 4 days (a, a′) 10:0; (b, b′) 6:4; (c, c′) 5:5.

ure 3 shows the fiber morphologies of the samples after treatment with 75% (v/v) ethanol vapor and water-resistance test. Compared with electrospun SF/HA fibers (Fig. 1), the fiber morphologies showed no significant change after treatment. For

the water-resistance test, the nanofibrous structure was still preserved after being soaked in deionized water for 4 days. The results indicated that 75% (v/v) ethanol vapor can effectively treat electrospun SF/HA fibers. In our experiment, we found 75% (v/v) ethanol vapor treatment processing was also a kind of effective sterilization approach to SF and SF/HA nanofiber scaffolds. Treated nanofibrous scaffolds did not need further complicated sterilization processing. Therefore, 75% (v/v) ethanol vapor treatment was an ideal post-treatment for SF and SF/HA nanofibrous scaffolds.

3.3. Structure Analyses of SF/HA Nanofibers

SF has characteristic absorption bands at 1650–1660 (amide I), 1535–1545 (amide II), 1235 (amide III) and 669 cm^{-1} (amide V), attributed to the SF with random coil or α-helix conformation (silk I), and characteristic bands at 1625–1640, 1515–1525, 1265 and 696 cm^{-1}, attributed to the SF with β-sheet conformation (silk II) [27, 28]. Figure 4 shows FT-IR spectra of electrospun SF, electrospun SF/HA nanofibers before and after being treated with 75% (v/v) ethanol vapor and raw HA. The electrospun SF showed absorption bands at 1651 (amide I), 1537 (amide II) and 1240 cm^{-1} (amide III), which were assigned to the SF with random coil conformation. The raw HA showed absorption bands at 1320, 1048, 1143 and 947 cm^{-1}, which were attributed to the saccharide structure, and at 1612, 1408, 1261 cm^{-1}, which were attributed to carboxylate groups. The band at 1613 cm^{-1} was assigned to carboxyl (C=O) stretching vibrations, the band at 1408 cm^{-1} was assigned to carboxyl (C–O) symmetric stretching vibrations [29].

The electrospun SF/HA nanofibers showed absorption bands at 1648 (amide I), 1533 (amide II) and 1240 cm^{-1} (amide III). These absorption bands showed no obvious difference in comparison with electrospun pure SF. The conformation of SF still existed in random coil or α-helix. The result clarified that HA did not induce SF conformation from random coil or α-helix to β-sheet. After being treated with 75% (v/v)ethanol vapor, the absorption bands at 1648 (amide I), 1533 (amide II) and

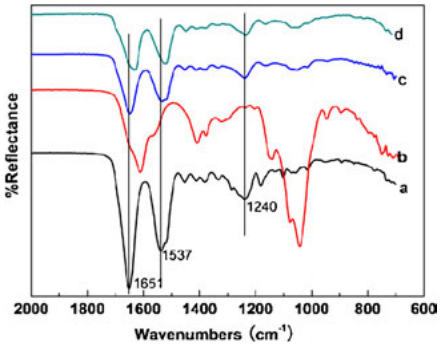

Figure 4. FT-IR–ATR spectra of (a) electrospun SF; (b) raw HA; (c) electrospun SF/HA (6:4); (d) electrospun SF/HA (6:4) after treatment with 75% (v/v) ethanol vapor. This figure is published in colour in the online edition of this journal, which can be accessed *via* http://www.brill.nl/jbs

1240 cm^{-1} (amide III) shifted to 1630, 1520 and 1234 cm^{-1}, which was attributed to the SF with β-sheet conformation (silk II). Therefore, 75% (v/v) ethanol vapor could transform the crystal structure of SF from silk I (soluble in water) to silk II (insoluble in water).

Recently, solid-state ^{13}C-NMR has been shown to be an effective analytical tool for demonstrating the formation of β-sheets in polypeptides and proteins due to the sensitivity of isotropic ^{13}C-NMR chemical shifts of carbon atoms to the secondary structure. The secondary structure of *Bombyx mori* SF consists of the major conformations including random coils or helix (silk I) and β-sheet (silk II) [28]. The β-sheet form can be identified by the ^{13}C chemical shifts of Gly (glycine), Ser (serine) and Ala (alanine) that are indicative of β-sheet conformations. Particularly, the chemical shift of alanyl C^{β} is an excellent indicator of the silk fibroin conformation. The literatures reported the chemical shifts in Ala residues of C^{β} within 18.5–20.5 ppm and in Ala residues of C^{α} within 48.6–49.7 ppm were assigned to β-sheet conformation (silk II), the chemical shifts in Ala residues of C^{β} within 14.5–17.5 ppm and in Ala residues of C^{α} within 49.7–52.6 ppm were assigned to random coils or helix (silk I) [30]. The ^{13}C/NMR spectra of electrospun SF scaffolds, raw HA and electrospun SF/HA scaffolds are shown in Fig. 5A. In the ^{13}C-NMR spectra of pure SF nanofibrous scaffolds, peaks at 172.0, 61.2, 51.0, 16.3 and 42.5 ppm were assigned to carbonyl carbons of SF, C^{β} of Ser, C^{α}, C^{β} of Ala and C^{α} of Gly [31]. In the ^{13}C-NMR spectra of raw HA, the peaks at 174.4, 102.2, 75.2 and 55.8 ppm were attributed to carbonyl carbons of HA, C1, C4/C5 and C2 of HA [32]. The ^{13}C-NMR spectra of SF/HA blended nanofibrous scaffolds showed characteristics chemical shifts of both SF and HA and the chemical shifts of C^{α} and C^{β} of Ala were 53.8 and 16.4 ppm, which were assigned to random coils or helix

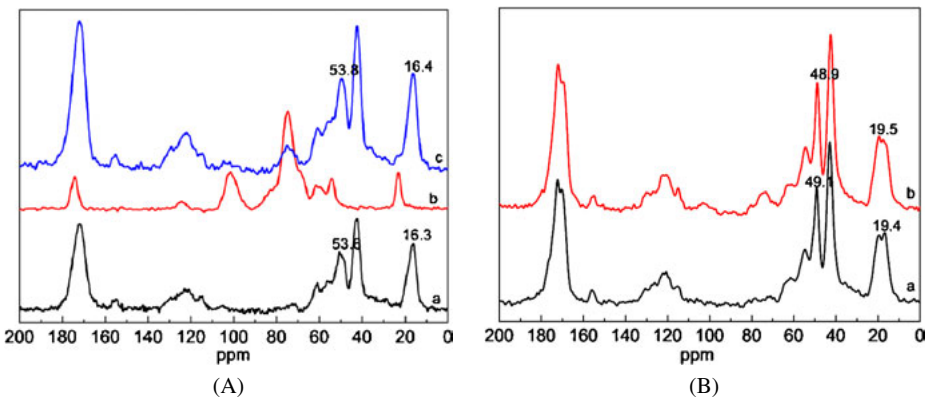

Figure 5. (A) ^{13}C-NMR spectra of (a) electrospun SF; (b) raw HA; (c) electrospun SF/HA (6:4). (B) ^{13}C-NMR spectra of (a) electrospun SF and (b) electrospun SF/HA (6:4) nanofibers after being treated with 75 v/v% ethanol vapor. This figure is published in colour in the online edition of this journal, which can be accessed *via* http://www.brill.nl/jbs

(silk I). The results suggested HA did not induce conformation of SF to transform from random coil to β-sheet structure.

The ^{13}C-NMR spectra of the electrospun SF scaffolds and electrospun SF/HA scaffolds after treatment with 75% (v/v) ethanol vapor are shown in Fig. 5B. After treatment with the 75% (v/v) ethanol vapor, the chemical shifts of C^{α} and C^{β} of Ala were 49.1 and 19.4 ppm, and the peak at 172.3 ppm for carbonyl carbon split into a doublet in electrospun SF scaffolds. The chemical shifts of C^{α} and C^{β} of Ala were 48.6 and 19.5 ppm, and the peak at 172.3 ppm for carbonyl carbon split into doublet in electrospun SF/HA scaffolds, which clearly indicated that 75% (v/v) ethanol vapor could transform SF conformation from random coil to β-sheet structure (silk II). Meanwhile, the chemical shifts of C^{β} of Ala had different shape of the peak in SF and SF/HA scaffolds. We calculated the content of β-sheet conformation of SF/HA scaffolds and SF scaffolds after treatment with 75% (v/v) ethanol vapor. The β-sheet content of SF/HA scaffolds was higher than that of SF scaffolds. HA could promote folding of SF from random coil into β-sheet structure in the presence of 75% (v/v) ethanol vapor.

The thermographs of electrospun SF, electrospun SF/HA nanofibers before and after treatment with 75% (v/v) ethanol vapor are shown in Fig. 6. The samples exhibited an endothermic peak at around 80°C, which was attributed to the evaporation of water. For the electrospun SF scaffolds, the appearance of an endothermic peak at 178.1°C was due to the glass transition of amorphous SF. The small exothermic peak at 232.2°C was due to crystallization of amorphous SF with the accompanying conformation transition from random coil to β-sheet [33]. For the electrospun SF/HA scaffolds, the endothermic peaks at 178.9°C for the glass transition of amorphous SF still appeared but no exothermic peak for crystallization of amorphous SF was observed until the decomposition temperature. This was caused by HA not inducing SF conformation from random coil to β-sheet. Meanwhile, the H-bond interaction between HA and SF molecules may hinder folding of SF

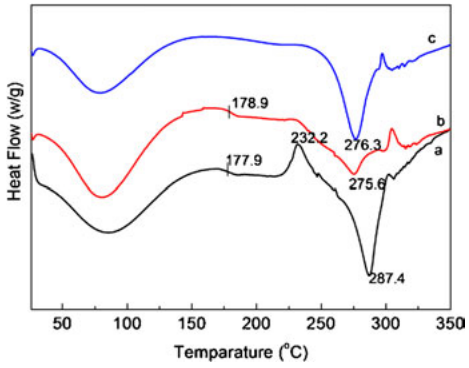

Figure 6. The thermographs of (a) electrospun SF; (b) electrospun SF/HA (6:4); (c) electrospun SF/HA (6:4) after treatment with 75% (v/v) ethanol vapor. This figure is published in colour in the online edition of this journal, which can be accessed *via* http://www.brill.nl/jbs

molecules into β-sheet structure in heat process. For the electrospun SF/HA scaffolds treatment with 75% (v/v) ethanol vapor, peaks both for the glass transition and for crystallization disappeared. The reason was their initial structures were β-sheet. The samples exhibited endothermic peaks at around 280°C, which was attributed to the decomposition of SF. The adding of HA led to a slight decrease of the decomposition temperature. The thermoanalytical results were consistent with the results from the NMR and FT-IR characterization studies.

3.4. Viablity Study of Cells on Nanofibrous Scaffolds

ECM consists of a nanoscale fibrous network of proteins and proteoglycans. The topographical cues of electrospinning naofibers may have significant influence on cell adhesion and proliferation. To evaluate cell adhesion and proliferation on the electrospun SF/HA nanofibrous scaffolds. The viability of PIECs on days 1, 3, 5 and 7 after seeding on various nanofiberous scaffolds was studied and shown in Fig. 7. The nanofibrous scaffolds showed a highly significant increase ($P < 0.01$) compared with cover slips on days 1, 3, 5 and 7. The results revealed that all the nanofibrous scaffolds had greater cell viability in comparison with coverslips. On day 1, proliferation on SF/HA (6:4) and SF/HA (5:5) nanofiberous scaffolds exhibited a significant decrease ($P < 0.05$) compared to TCP. However, on days 3, 5 and 7, all nanofibrous scaffolds showed no significant difference as compared to TCP, and there was no significant difference among different nanofibrous scaffolds. The results showed pure SF and SF/HA blended nanofibrous scaffolds could greatly promote cell growth and proliferation.

Cell morphology and the interaction between cells and pure SF and SF/HA nanofibrous scaffolds were studied *in vitro* for 3 days, as shown in Fig. 8. It revealed that PIECs could attach and spread on pure SF, SF/HA with different volume ratios nanofibrous scaffolds. Therefore, SF/HA nanofibrous scaffolds to biomimic the ECMs might be beneficial to cell growth for tissue-engineering application.

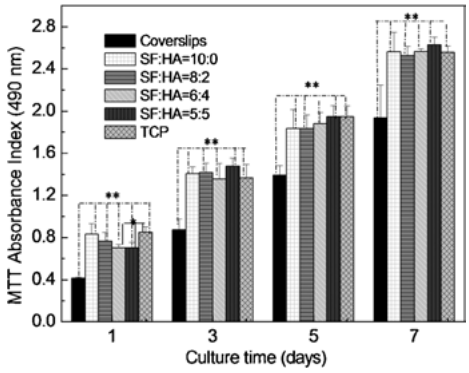

Figure 7. Proliferation of PIECs cultured on SF/HA nanofibrous scaffolds, coverslips and TCP for 1, 3, 5, 7 days. Data are expressed as mean ± SD ($n = 3$). Statistical difference between groups is indicated ($^{*}P < 0.05$; $^{**}P < 0.01$).

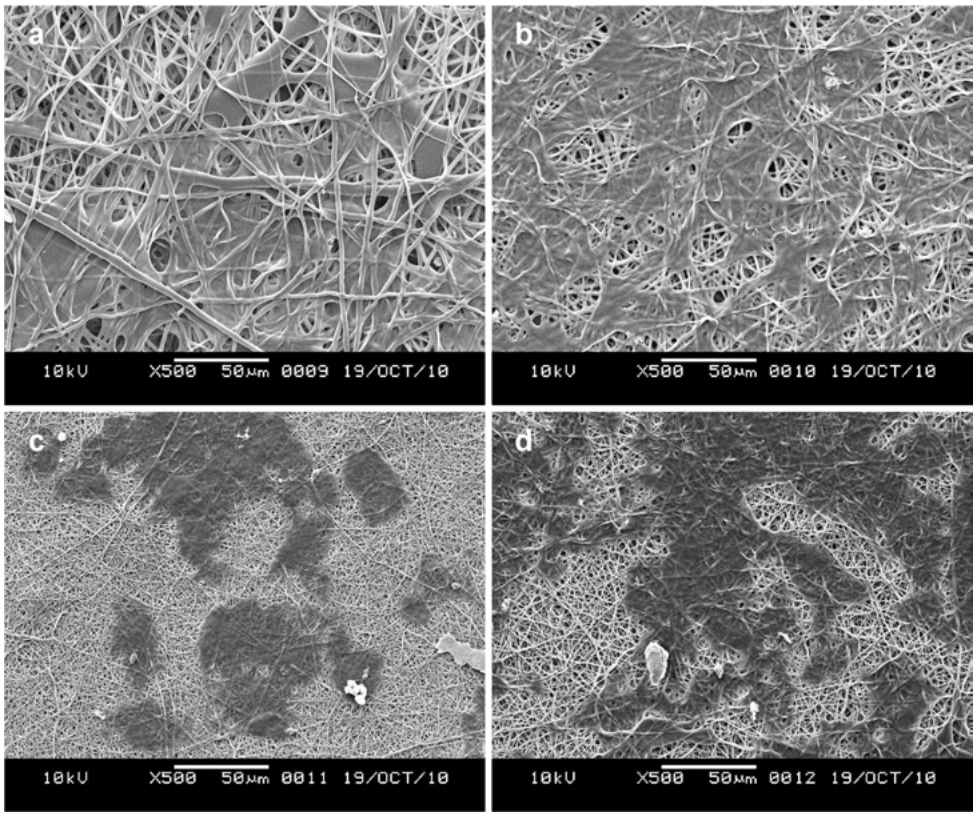

Figure 8. SEM micrographs of PIECs grown on nanofibrous scaffolds for 3 days. (a) 10:0; (b), 8:2; (c), 6:4; (d), 5:5.

4. Conclusion

HA and *Bombyx mori* SF are an abundant polysaccharide and protein in nature. To further biomimic topological structure and chemical composition of natural ECMs, electrospun nanofibrous scaffolds of SF/HA were fabricated from aqueous solutions at the first time. Treatment with 75% (v/v) ethanol vapor could not only lead to conformation of SF from random coil or α-helix to β-sheet structure, but also become effective sterilization approach to electrospun SF and SF/HA nanofibrous scaffolds. Cell behavior on nanofibrous scaffolds demonstrated that cells proliferated well on the SF/HA nanofibrous scaffolds. For cytocompatibility, though there are no salient difference as compared to elecrospun SF nanofibrous scaffolds, the addition of HA could better biomimick the chemical composition than pure SF; therefore, electrospun SF/HA nanofibrous scaffolds may be more conducive to tissue regeneration, Ongoing studies will focus on tissue engineering application or serving as vehicle for water-soluble drugs.

Acknowledgements

This research was supported by the Science and Technology Commission of Jiaxing Municipality Program (2010AY1089), The Key Program of Jiaxing University (70110X10BL), National High Technology Research and Development Program (863 Program, 2008AA03Z305), National Natural Science Foundation of China (51073072), the Zhejiang Provincial Natural Science Foundation (Y4100745) and the Science and Technology Department of Zhejiang Province (2010C01020).

References

1. J. Lannutti, D. Reneker, T. Ma, D. Tomasko and D. Farson, *Mater. Sci. Eng. C* **27**, 504 (2007).
2. S. Sell, C. Barnes, M. Smith and M. McClure, *Polym. Int.* **56**, 1349 (2007).
3. B. M. Min, G. Lee, S. H. Kim, Y. S. Nam, T. S. Lee and W. H. Park, *Biomaterials* **25**, 1289 (2004).
4. M. Wang, H. J. Jin, D. L. Kaplan and G. C. Rutledge, *Macromolecules* **37**, 6856 (2004).
5. W. J. Li, C. T. Laurencin, E. J. Caterson, R. S. Tuan and F. K. Ko, *J. Biomed. Mater. Res.* **60**, 613 (2002).
6. S. A. Sell, M. J. McClure, K. Garg, P. S. Wolfe and G. L. Bowlin, *Adv. Drug Deliv. Rev.* **61**, 1007 (2009).
7. K. Y. Lee, L. Jeong, Y. O. Kang, S. J. Lee and W. H. Park, *Adv. Drug Deliv. Rev.* **61**, 1020 (2009).
8. S. S. Liao, B. J. Li, Z. W. Ma, H. Wei, C. Chanand and S. Ramakrishna, *Biomed. Mater.* **1**, 45 (2006).
9. M. Santin, A. Motta, G. Freddi and M. Cannas, *J. Biomed. Mater. Res.* **46**, 382 (1999).
10. R. L. Horan, K. Antle, A. L. Collette, Y. Z. Huang, J. Huang, J. E. Moreau, V. Volloch, D. L. Kaplan and G. H. Altman, *Biomaterials* **26**, 3385 (2005).
11. X. H. Zhang, M. R. Reagan and D. L. Kaplan, *Adv. Drug Deliv. Rev.* **61**, 988 (2009).
12. Y. M. Yang, F. Ding, J. Wu, W. Hu, W. Liu, J. Liu and X. S. Gu, *Biomaterials* **28**, 5526 (2007).
13. S. M. Kuo, Y. J. Wang, G. C. Niu, H. E. Lu and S. J. Chang, *J. Mater. Sci. Mater. Med.* **19**, 1235 (2008).
14. M. Garcia-Fuentes, A. J. Meinel, M. Hilbe, L. Meinel and H. P. Merkle, *Biomaterials* **30**, 5068 (2009).
15. M. C. Yang, N. H. Chi, N. K. Chou, Y. Y. Huang, T. W. Chung, Y. L. Chang, H. C. Liu, M. J. Shieh and S. S. Wang, *Biomaterials* **31**, 854 (2010).
16. S. Zarkoob, R. K. Eby, D. H. Reneker, S. D. Hudson, D. Ertley and W. W. Adams, *Polymer* **45**, 3973 (2004).
17. Y. Kawahara, A. Nakayama, N. Matsumura, T. Yoshioka and M. Tsuji, *J. Appl. Polym. Sci.* **107**, 3681 (2008).
18. K. Ohgo, C. H. Zhao, M. Kobayashi and T. Asakura, *Polymer* **44**, 841 (2003).
19. S. Sukigara, M. Gandhi, J. Ayutsede, M. Micklus and F. Ko, *Polymer* **44**, 5721 (2003).
20. C. Chen, C. B. Cao, X. L. Ma, Y. Tang and H. S. Zhu, *Polymer* **47**, 6322 (2006).
21. K. H. Zhang, X. M. Mo, C. Huang, C. H. He and H. S. Wang, *J. Biomed. Mater. Res. A* **93**, 976 (2010).
22. I. C. Um, D. F. Fang, B. S. Hsiao, A. Okamoto and B. Chu, *Biomacromolecules* **5**, 1428 (2004).
23. S. Koombhongse, W. X. Liu and D. H. Reneker, *J. Polym. Sci. Part B: Polym. Phys.* **39**, 2598 (2001).
24. X. H. Zong, K. Kim, D. F. Fang, S. F. Ran, B. S. Hsiao and B. Chu, *Polymer* **43**, 4403 (2002).
25. L. Jeong, K. Y. Lee, J. W. Liu and W. H. Park, *Int. J. Biol. Macromol.* **38**, 140 (2006).

26. B. M. Min, L. Jeong, K. Y. Lee and W. H. Park, *Macromol. Biosci.* **6**, 285 (2006).
27. J. Magoshi, M. Mizuide and Y. Magoshi, *J. Polym. Sci. Polym. Phys. Edn* **17**, 515 (1979).
28. X. Chen, Z. Z. Shao, N. S. Marinkovic, L. M. Miller, P. Zhou and M. R. Chance, *Biophys. Chem.* **89**, 25 (2001).
29. K. Haxaire, Y. M. Chal, M. Milas and M. Rinaudo, *Biopolymers (Biospectroscopy)* **72**, 10 (2003).
30. P. Zhou, G. Y. Li, Z. Z. Shao, X. Y. Pan and T. Y. Yu, *J. Phys. Chem. B* **105**, 12469 (2001).
31. T. Asakura, M. Iwadate, M. Demura and M. P. Williamson, *Int. J. Biol. Macromol.* **24**, 167 (1999).
32. C. D. Meo, D. Capitani, L. Mannina, E. Brancaleoni, D. Galesso, G. D. Luca and V. Crescenzi, *Biomacromolecules* **7**, 1253 (2006).
33. J. Magoshi, Y. Magoshi, S. Nakamura, N. Kasai and M. Kakudo, *J. Polym. Sci.: Polym. Phys. Edn* **15**, 1675 (1977).